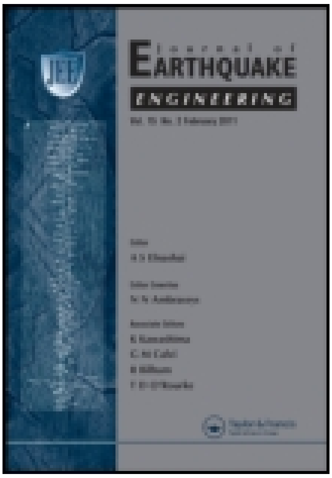

Journal of Earthquake Engineering
Publication details, including instructions for authors and subscription information:
http://www.tandfonline.com/loi/ueqe20

Experimental Study of New Seismic Protective Devices for Low-Rise Steel Buildings

Paul Kohan [a] , Daniel Wendichansky [b] & Luis E. Suarez [b]

[a] Facultad de Ingeniería , Universidad Nacional de Salta , Salta , Argentina

[b] Civil Engineering and Surveying Department , University of Puerto Rico , Mayaguez , Puerto Rico

Published online: 28 Dec 2011.

Journal of Earthquake Engineering, 16:83–104, 2012

ISSN: 1363-2469 print / 1559-808X online
DOI: 10.1080/13632469.2011.576800

Taylor & Francis
Taylor & Francis Group

Experimental Study of New Seismic Protective Devices for Low-Rise Steel Buildings

PAUL KOHAN[1], DANIEL WENDICHANSKY[2], and LUIS E. SUAREZ[2]

[1]Facultad de Ingeniería, Universidad Nacional de Salta, Salta, Argentina
[2]Civil Engineering and Surveying Department, University of Puerto Rico at Mayaguez, Mayaguez, Puerto Rico

The effectiveness of four protective systems in reducing the seismic structural response is assessed via shaking table tests using a 1/6-scale model of a steel building. The protective systems consist of two cables connected to hanging weights and to the top of the structure. The cables move guided by pulleys mounted on auxiliary structures. The devices dissipate energy through friction and in some variants also by impact with the ground. The tests show that the systems were capable of producing significant reductions in floor displacements and bending moments. The accelerations were also reduced, albeit not at the same level.

Keywords Passive Systems; Protective Systems; Retrofitting; Shaking Table Tests; Steel Buildings

1. Introduction

Under current seismic design practices, the structural systems are generally designed to respond beyond the elastic limit during strong earthquakes. The seismic provisions included in the codes allow for the development of mechanisms that involve ductile inelastic response in specific regions of the structural system. Although in part due to its relatively low initial cost, seismic design based on inelastic response is attractive, it is likely that during moderate earthquakes some zones of the lateral force resisting system of the structure will be damaged and will need repair, whereas during severe earthquakes they may be damaged beyond repair. While the principle of mitigating loss of life during a strong earthquake still prevails, resilient communities require structures that can survive a moderate or severe earthquake with relatively little disturbance to their functions. The cost associated with the loss of business operation and the damage to buildings content, expensive equipment, and non structural components following an even moderate earthquake can be comparable to, if not greater than, the cost of the structure itself. Therefore, ideally, repairs requiring loss of business continuity should be avoided in strong events. The situation is even more stringent for schools and other buildings used for critical operations such as hospitals, police stations and fire departments that must remain fully functional (i.e., with minimum or no damage) during and after the seismic shakings. These issues have led to the development in the last decades of innovative control systems, sometimes referred to as structural protective systems or earthquake protective systems. These systems are usually classified into three

Received 27 June 2010; accepted 28 March 2011.
Address correspondence to Luis E. Suarez, Civil Engineering and Surveying Department, University of Puerto Rico at Mayaguez, Mayaguez, PR 00681-9000; E-mail: luis.suarez3@upr.edu

groups: (1) Passive systems, including base isolation systems; (2) semi-active or hybrid systems; and (3) active systems.

Among all structural control devices, the passive systems, along with base isolation, became the most accepted by the structural engineering community and the construction industry and thus the number of buildings and bridges fitted with these systems continues to grow. Although the passive devices have the drawback that they cannot achieve the level of response reductions of active or semi-active systems, they are less expensive and reliable as they do not require specialized software, actuators, sensors and an energy supply. The analysis and design of these devices is now well understood and described in a few monographs and books [Soong, 1990; Soong and Dargush, 1997; Hanson and Soong, 2001; Christopoulos and Filiatrault, 2006; Cheng *et al*., 2008].

Most of the passive systems are devised to somehow enhance the energy dissipation characteristics of the structure. This is done by using several phenomena such as frictional sliding, shear deformation of viscoelastic materials, viscous fluid orificing, yielding of metals, and phase transformation in metals [Soong and Spencer, 2002].

In this article, four new retrofitting mechanisms to improve the response of steel structures to earthquakes motions are proposed and compared. These mechanisms are based on modifications of the same general device which use the friction produced on a pulley system as the energy dissipator source, resulting on a very simple and economic method.

In order to analyze the effectiveness of the mechanisms proposed, a $1/6$ scale model of a steel structure typical of commercial buildings in Puerto Rico was built. The scale model fitted with different configurations of the original device was subjected to a set of simulated earthquake tests on a shaking table. The model was defined following the similitude laws derived from the Artificial Mass Simulation Method [Moncarz and Krawinkler, 1981]. The main variables considered in the analysis were the absolute acceleration and relative displacements of selected points at different levels and the internal forces in the columns of the first level. The protective devices can be used to retrofit deficient buildings or incorporated into new constructions.

2. Development of the Scale Model

2.1. Prototype Definition

The prototype structure was selected based on a survey of industrial and commercial steel buildings constructed in Puerto Rico [Kohan, 2007]. These are mostly low-rise structures constructed between the mid-1960s and the mid-1980s; they were designed for lateral forces that in certain cases substantially lower than those prescribed in the current codes. The structure chosen is a two-story steel spatial frame, with two bays in one direction and one bay in the other direction. Its layout is shown in Fig. 1a. The story height is 4.57 m and the bay length is 6.93 m. The beams and columns of the prototype structure were selected from commercial shapes: standard sections W12x96 were adopted for the columns and W21x40 for the beams. The structure is assumed to be built on stiff rock conditions so that no soil-structure interaction or differential settlements need to be considered. The weights of the elements (columns, beams, and floor system) of the prototype, per level and total, are shown in Table 1.

2.2. Model Definition

It was set as one of the goals of the study to build and test the largest possible steel model that could be accommodated on the shaking table of the University of Puerto

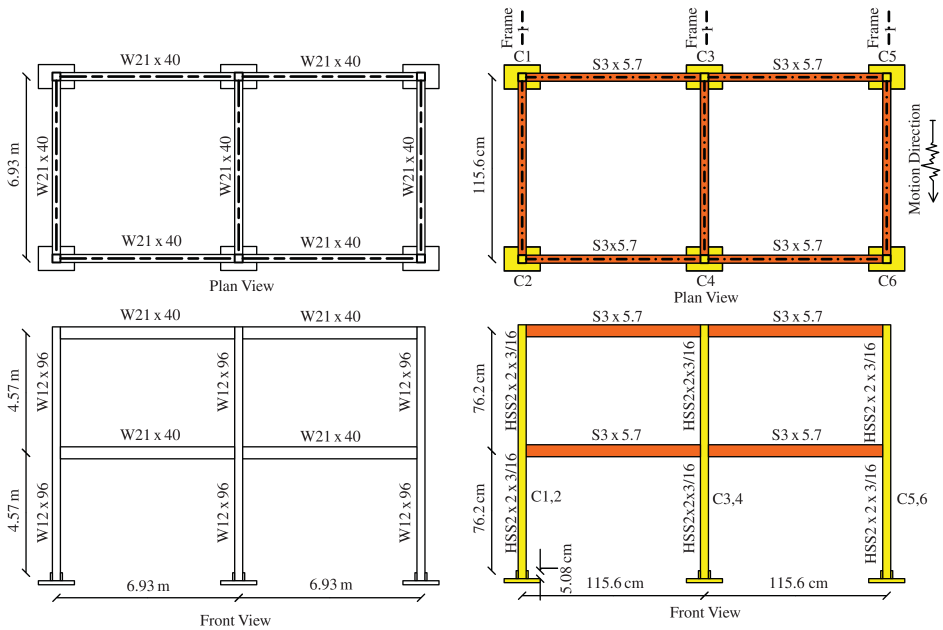

(a) Prototype Layout (b) Scale Model Layout

FIGURE 1 General layout: (a) prototype and (b) scale model (color figure available online).

TABLE 1 Prototype weight

	First level (KN)	Second level (KN)
Beams	44.0	44.0
Columns	38.3	19.1
Floor System	202.8	202.8
Total	285.1	265.9

Rico at Mayagüez. Taking into account the size constraints and the load capacity of the shaking table, a one-sixth (1/6) scale was adopted. The relatively small, one-directional electro-hydraulic shaking table was constructed in 2005 [Cortés-Delgado, 2005].

The general layout of the 1/6 scale model structure is shown in Fig. 1b. Figure 2 shows photographs of the model constructed and mounted on the shaking table taken from two standpoints. The story height of the model is 76.2 cm for both levels, and the bays length is 115.6 cm. All the beam-to-column connections are flexible, and therefore the moment transfer is minimized. All the columns are continuous and they are rigidly attached to the base (i.e., to the shaking table); only the beams have pinned connections.

Four additional W10×33 steel beams were added as extra supports to enlarge the shaking table dimensions. These supports allowed for the use of a scale model larger than the original platform of the shaking table. However, they also introduced some flexibility into the system producing some asymmetric response of the model, as will be shown later.

The properties of the structural shapes used in the construction of the scale model are summarized in Table 2. The properties of the bars necessary to satisfy the moment of inertia and cross-sectional area imposed by similitude requirements are presented in columns 3

FIGURE 2 The model on the shaking table (color figure available online).

TABLE 2 Summary of the prototype and model sections properties

	Column			Beam		
	Prototype	Model: required	Model: provided	Prototype	Model: required	Model: provided
Shape	W12×96	N/A	HSS2×2×3/16	W21×44	N/A	S3×5.7
Inertia (cm^4)	1,443,162	1,107.19	1,111.34	1,460,485	1,127.99	4,382.92
Area (cm^2)	1,173.5	32.26	49.68	499.4	14.84	69.68

and 6 of Table 2. Columns 4 and 7 of the table show the actual geometric properties provided by the sections adopted. Since the response of this model is more influenced by the moment of inertia of the columns than by its cross sectional geometry and area, some variation in these parameters can be tolerated [Mills *et al.*, 1979]. Therefore, HSS 2×2×3/16 shapes were used for columns, instead of W-shapes. Moreover, since the beam-to-column connections were flexible, it was reasoned that neither the area nor the moment of inertia of the beams would affect significantly the general behavior of the model, and hence standard shapes S 3 × 5.7 were used for the beams.

The selection of flexible connections merits a clarification. The proposed protective systems (to be described later) are intended for use in two situations. First, they can be regarded as an alternative to available passive retrofitting systems to attenuate the seismic response of *existing* structures with this type of connections. This situation could arise, for instance, in a structure where the lateral resisting system was originally designed as a moment resisting frame but for some reason (e.g., construction mistakes, damage caused by medium intensity earthquakes) the beam-to-column connections do not have the required rigidity. The scale model used in the project represents the most unfavorable condition, i.e., where the beams and columns are flexible (i.e., approximately pin-connected). In the second case, the proposed protective systems could be incorporated at the design stage of *new structures* with moment resisting frames. In this, case the structural elements of the frames and their connections could be designed for stresses lower than those expected in the bare (non retrofitted) structure. Again, here the scale model used in the present study represents the least favorable condition.

To satisfy mass similitude requirements, in addition to the self-weight of the model, additional weight must be added [Bracci *et al.*, 1992]. The weight of the bare model assigned to each level (W_m^{prov}) due to the structural elements is shown in Table 3. The weight required (W_m^{req}) to satisfy similitude requirement for gravitational forces was

TABLE 3 Summary of the additional weights requirement

	Weight required W_m^{req} (kN)	Weight provided W_m^{prov} (kN)	Weight to be added $\Delta W = W_m^{req} - W_m^{prov}$ (kN)
First level	7.92	1.22	6.70
Second level	7.39	1.05	6.34

FIGURE 3 View of the added steel plates (color figure available online).

determined as the weight of the prototype (W_p) divided by the gravitational forces scale law ($\lambda_F = \lambda_L^2 = 36$). The weight required to be added to each level of the model is presented in Table 3.

In order to account for the weight deficiency, steel plates were added to each level. Each of the plates, shown in Fig. 3, was 116.8 cm long, 15.2 cm wide, and 1.6 cm thick, and weighted 222.4 N. Therefore, to obtain the approximately 6.3 kN per floor required, 28 plates were placed at each level. There was no connection between the plates and they were simply supported by the beams; thus no rigid diaphragm was created.

2.3. Model Instrumentation

The response quantities selected to study the performance of the different protective schemes were the absolute accelerations at three points on the two floors, the relative displacements at three points on the second floor, and the internal forces in four columns of the first floor. Linear variable differential transformers (LVDT), piezoresistive accelerometers, and force transducers (load cells) were installed in the scale model. The general layout of the instrumentation used is shown in Fig. 4. There are four displacement sensors: three at the second floor level—identified as LVDT1, LVDT2, and LVDT3—and one at the base (shaking table) level, designated as LVDT0. Six uniaxial accelerometers were installed in the test structure in the direction of the base acceleration. The accelerometers at the first level were identified as A11, A21, and A31, and those at the second level are A12, A22,

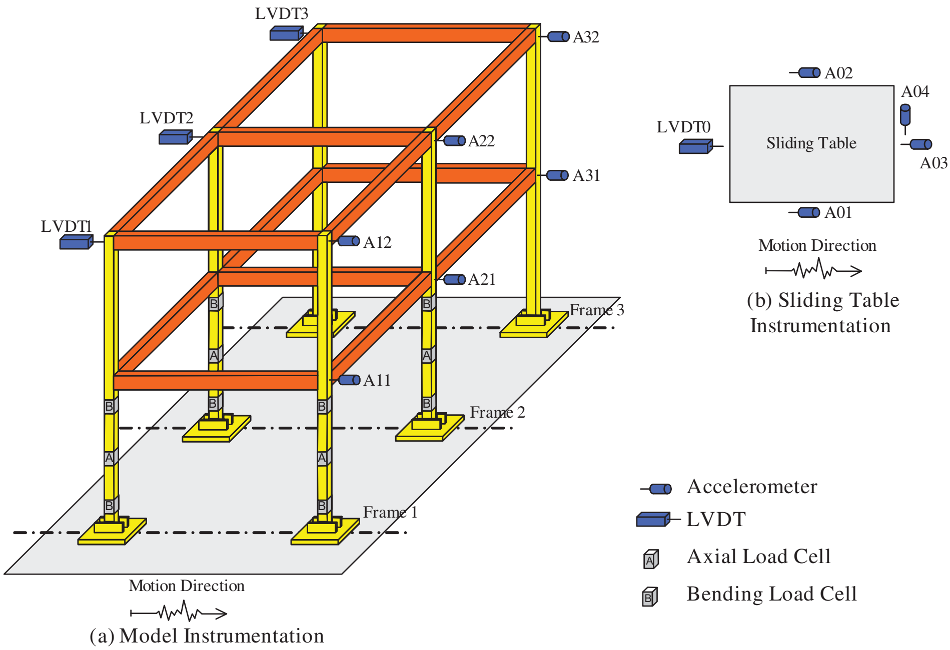

FIGURE 4 Layout of the instrumentation (color figure available online).

and A32. In addition, four accelerometers were placed in the shaking table as shown in Fig. 4b. Three accelerometers, identified as A01, A02, and A03, measure the acceleration of the shaking table in the direction of motion, and a fourth accelerometer, designated as A04, was used to record the acceleration in the normal direction.

Special force transducers (load cells) were installed in four of the six first-story columns (columns 1 and 2 of Frame 1, and columns 3 and 4 of Frame 2) to measure the internal forces in the model. Two load cells at the top and bottom of each column measured the bending moment in the direction of the motion, and one in the middle of the columns measures the axial force. Axial and bending moment load cells were based on different arrangements of Wheatstone bridge circuits. In both cases, full bridges were chosen to improve the output signal.

3. Description of the Retrofitting Schemes

It was mentioned that the main objective of this article was to propose and test different devices that can be used as retrofitting schemes to improve the response of steel structures to earthquakes motions. Three main conditions were imposed to devise the protective system.

(i) The system should not block the internal circulation of the building (i.e., it must be not invasive), and therefore it should be applied externally (or in an existing internal core).
(ii) The system should consist of a simple mechanism such that no further calibration after installation is required, nor special materials should be needed for its construction.
(iii) Tthe system should not be expensive.

Four retrofitting mechanisms that satisfy the above requirements were proposed. They are based on variations of a same general set up, which is shown schematically in Fig. 5.

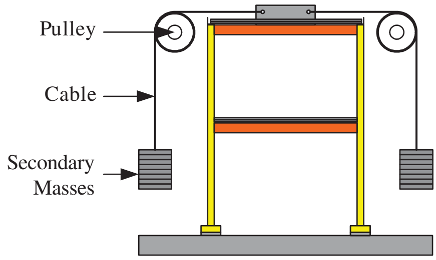

FIGURE 5 General set up of the protective system (color figure available online).

The fundamental passive protective system consists of two secondary masses connected to the second floor of the two-story building (in the case of the model used in the present study) by two cables passing through a pulley system. The pulleys are supported by rigid auxiliary structures disconnected from the building (not shown in Fig. 5 and described later). One of the ends of each cable is attached to the top of the structure, i.e., there is no continuity between them.

By modifying the basic configuration, it is possible to generate different retrofitting alternatives that will behave in various fashions. These retrofitting alternatives are summarized in Fig. 6 and are described next. For simplicity, the building structure is represented in Fig. 6 by a mass *M* supported by a single column.

Scheme 1. Free Pulley with a Hanging Mass System (FP)
In this alternative, the secondary masses were hanging from the cables and the pulleys were allowed to rotate. The cable used was practically inextensible, and thus when the system was excited the three masses (the secondary masses and the building mass) experienced the same displacements through time.

Scheme 2. Restrained Pulley with a Hanging Mass System (RP)
This alternative had the same layout than the FP system, but the pulleys were fixed, so no rotation was allowed. Therefore, friction forces were generated between the cable and the pulleys.

Scheme 3. Free Pulley with Ground Supported Masses (FPSM)

System	Schematic representation	Energy dissipation system
FP: Free Pulley	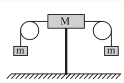	Internal friction in the axle bearings
RP: Restrained Pulley	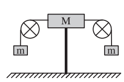	Friction between the cable and the pulleys
FPSM: Free Pulley - Ground Supported Masses	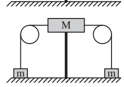	Pounding between the secondary masses and floor
RPSM: Restrained Pulley - Ground Supported Masses	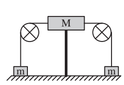	Friction between cable and pulleys and pounding

FIGURE 6 Summary of the retrofitting schemes studied.

In this alternative the secondary masses *m* were initially resting at the ground level. The pulley shafts were allowed to rotate. When the system was excited, one of the secondary mass was raised and when the earthquake motion reversed, this mass hit the floor in an alternate fashion. An amount of energy was lost in each collision. This alternative makes use of these collisions as a mechanism to dissipate energy.

Scheme 4. Restrained Pulley with Ground Supported Mass (RPSM)
This alternative is based on the previously described FPSM system but for this case the shafts of the pulleys were fixed.

The last two schemes with the impacting masses were intended as a preliminary concept. The idea is to compare them with the first two systems which were intended to be the primary candidates as protection devices. Therefore, the details regarding the implementation of schemes 3 and 4 will not addressed.

The selection of a scale model with two bays requires an explanation. Since the excitation is applied along one direction (see Fig. 4), at first sight it seems that it would be sufficient to use a one-bay model, or even a single plane frame with lateral supports to evaluate the performance of the retrofitting schemes. However, we wanted to assess whether it is necessary to install a protective device at each of the plane frames, or it is possible to mount only one system at one frame for the whole structure.

4. Scale Model Tests

Two types of tests were performed using the scale model in order to evaluate the effectiveness of the retrofitting alternatives proposed. The first tests were conducted to determine the dynamic properties of the scale model without the proposed protective devices. A white noise excitation was used for this case. The objective of the second tests was to analyze the response of the model fitted with the different devices subjected to earthquake motions.

Two series of simulated earthquake tests were performed to examine the effect of the secondary masses on the response. In the first set of tests, the secondary masses were equal to 10% of the mass of the model whereas in the second series the added masses were reduced to 5% of the structural mass.

5. Natural Frequencies and Modal Shapes

The natural frequencies and modal shapes of the bare model were obtained by running a series of tests using as input a white noise base acceleration. The frequency content of the signals used covered a range from 0–20 Hz. The first and second natural frequencies were identified at 4.47 Hz ($T_1 = 0.224$ s) and 15.51 Hz ($T_2 = 0.064$ s), respectively. The respective vibration modes are shown in Fig. 7. Note that there is a lack of symmetry in the modal displacements of the two external columns. As it was mentioned in a previous section, this effect was introduced by the additional beams installed on the shaking table platform to support a larger model.

The first mode shapes of the model with the different proposed retrofitting schemes are displayed in Fig. 8. The figure also shows the corresponding natural frequencies.

6. Simulated Earthquake Tests

6.1. Selection of the Earthquake Records

Acceleration records from four historical earthquakes were used to study the behavior of the structure equipped with the proposed protective schemes under different ground motions.

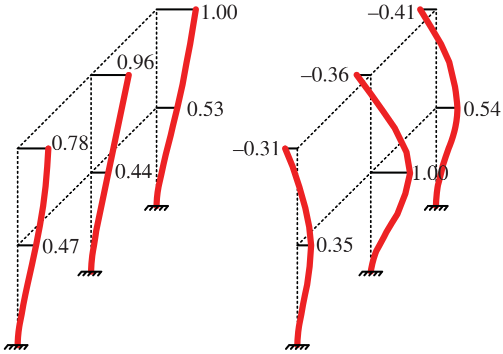

(a) 1st Mode f = 4.47 Hz (b) 2nd Mode f = 15.51 Hz

FIGURE 7 Modal shapes of the original scale model (color figure available online).

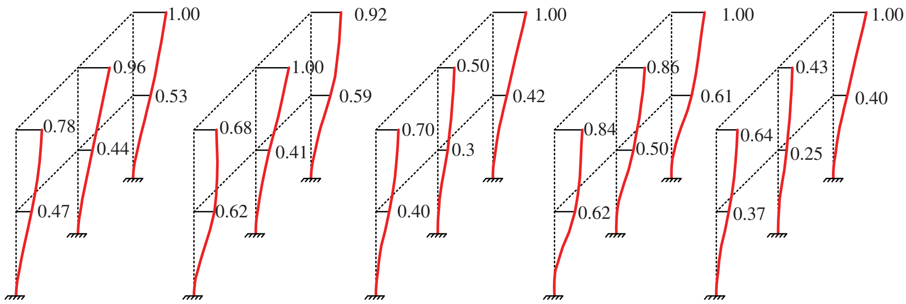

(a) BM f = 4.47 Hz (b) FP f = 4.25 Hz (c) RP f = 6.38 Hz (d) FPSM f = 4.40 Hz (e) RP f = 6.38 Hz

FIGURE 8 Modal shapes of the scale model with the protective devices (color figure available online).

The first two selected accelerograms were those of the 1940 Imperial Valley earthquake recorded at the El Centro station, and the 1952 Kern County earthquake registered at the Taft Lincoln School station. The response spectra of these records have been typically used in Puerto Rico in structural design for many years. In addition, the accelerograms of the 1994 Northridge earthquake recorded at the Castaic station and the 1986 San Salvador earthquake registered at the Hotel Camino Real station were selected. They were chosen among a selection made by Martínez-Cruzado *et al*. [2001] to generate new design spectra for Puerto Rico. They represent the type of records that could be expected in Puerto Rico based on similar fault characteristics, epicentral distances, etc. The main characteristics of the four earthquake records are displayed in Table 4.

TABLE 4 Characteristics of the accelerograms

Earthquake name and date	Station	Magnitude	PGA (g)
Imperial Valley, 18/5/1940	El Centro	7.0	0.313
Kern County, 21/7/1920	Taft Lincoln School	7.4	0.156
Northridge, 17/01/1994	Castaic	6.6	0.568
San Salvador, 10/10/1986	Hotel Camino Real	5.5	0.345

To satisfy time similitude requirements, a scale factor of $\lambda_t = \sqrt{\lambda_L}$ was used to compress the time variation of the accelerograms. The earthquake records were scaled to obtain a PGA equal to 0.3. However, the maximum accelerations measured at the platform in every test were slightly smaller. The difference in the PGA values might be due to accidental eccentricities and shaking table limitations.

6.2. Results from Simulated Earthquakes Tests

As shown in Fig. 9, two auxiliary structures were constructed to support the pulleys that make up the four proposed protective devices. These structures were attached to the shaking table but they were not connected to the primary structure.

It was observed during the tests that the two auxiliary masses had primarily a rectilinear motion (they moved up and down in the plane in which the base acceleration was applied). The two masses had a small pendular motion but it was not significant.

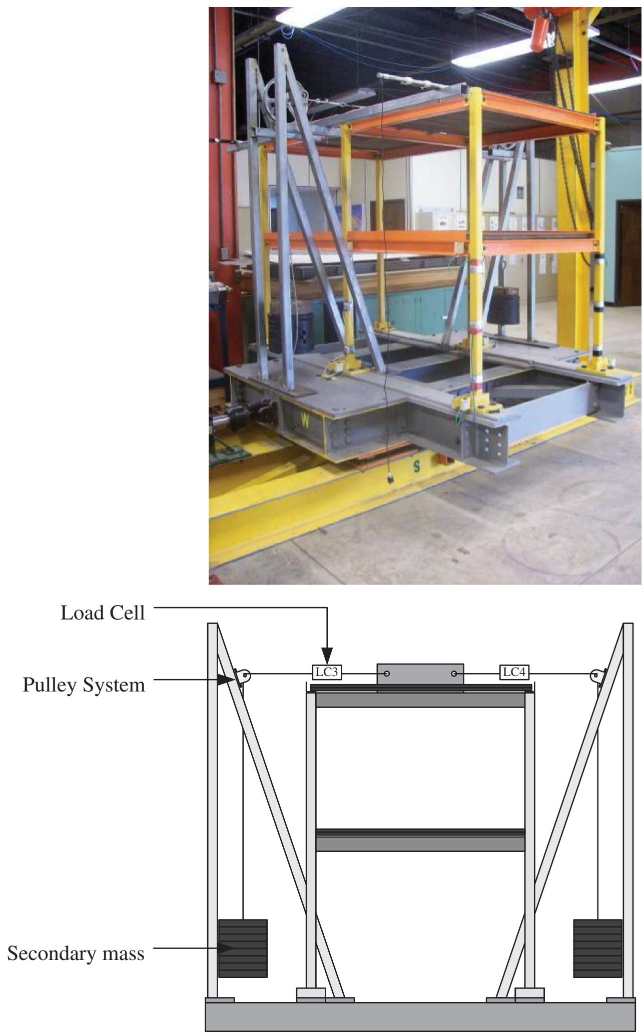

FIGURE 9 Set up of the model with secondary structures and protective devices (color figure available online).

TABLE 5 Peak accelerations from the El Centro test

		Peak accelerations (% g)						
Earthquake	Scheme	A11	A12	A21	A22	A31	A32	A02
EL Centro	BM	0.22	0.34	0.18	0.47	0.19	0.30	0.23
	FP	0.24	0.38	0.15	0.34	0.20	0.38	0.18
	RP	0.26	0.34	0.19	0.25	0.20	0.39	0.24
	FPSM	0.17	0.30	0.15	0.28	0.17	0.37	0.18
	RPSM	0.27	0.40	0.23	0.34	0.22	0.48	0.21

The response of the structure to the different base excitations was recorded using 24 sensors (LVDTs, accelerometers, and load cells) distributed over the model as shown in Fig. 4. Table 5 shows the peak absolute accelerations due to the scaled El Centro record measured by the six accelerometers installed in the two floors and the sensor at the base (A02). Table 6 displays the peak values of the relative displacements of the top floor recorded by the three displacement transducers. In both tables, the rows corresponding to the BM scheme show the responses obtained without any protective device (i.e., they correspond to the Bare Model). The results presented were obtained by using secondary masses with weights equal to 10% of the total weight of the model. Examining Table 6 it is evident that the four proposed devices were able to achieve a reduction in the displacements of the top floor. The pattern in the peak accelerations shown in Table 5 is more complicated: some of the schemes were able to reduce the accelerations but only at some locations. This situation will be discussed later.

The accelerations and relative displacements measured at the second level of the central frame of the building were considered to be the most relevant information among the measured response quantities, since in every test the highest peak accelerations and displacements of the bare model were measured at this node. Examining the response in Tables 5 and 6 one can conclude that the best overall results are obtained with the RP (fixed pulleys) alternative. It is relevant to point out that the reductions in displacement and acceleration occur during the entire duration of the excitation (i.e., they are not restricted to the peak values). This can be seen in the displacement time histories in Fig. 10 which were recorded during the test performed with the El Centro signal.

The results presented in Table 5 have interesting aspects that call for an explanation. It can be noticed that the peak accelerations of the joints at the beam-column connections of the bare model are slightly larger at the external joints (A11 and A31 for the 1st floor; A31 and A32 for the 2nd floor) than at the central joint (A21 and A22 for the 1st and 2nd floor,

TABLE 6 Peak relative displacements from the El Centro test

		Peak relative displacements (cm)		
Earthquake	Scheme	LVDT1	LVDT2	LVDT3
EL Centro	BM	0.46	0.76	0.71
	FP	0.41	0.71	0.58
	RP	0.25	0.20	0.38
	FPSM	0.25	0.46	0.51
	RPSM	0.30	0.25	0.53

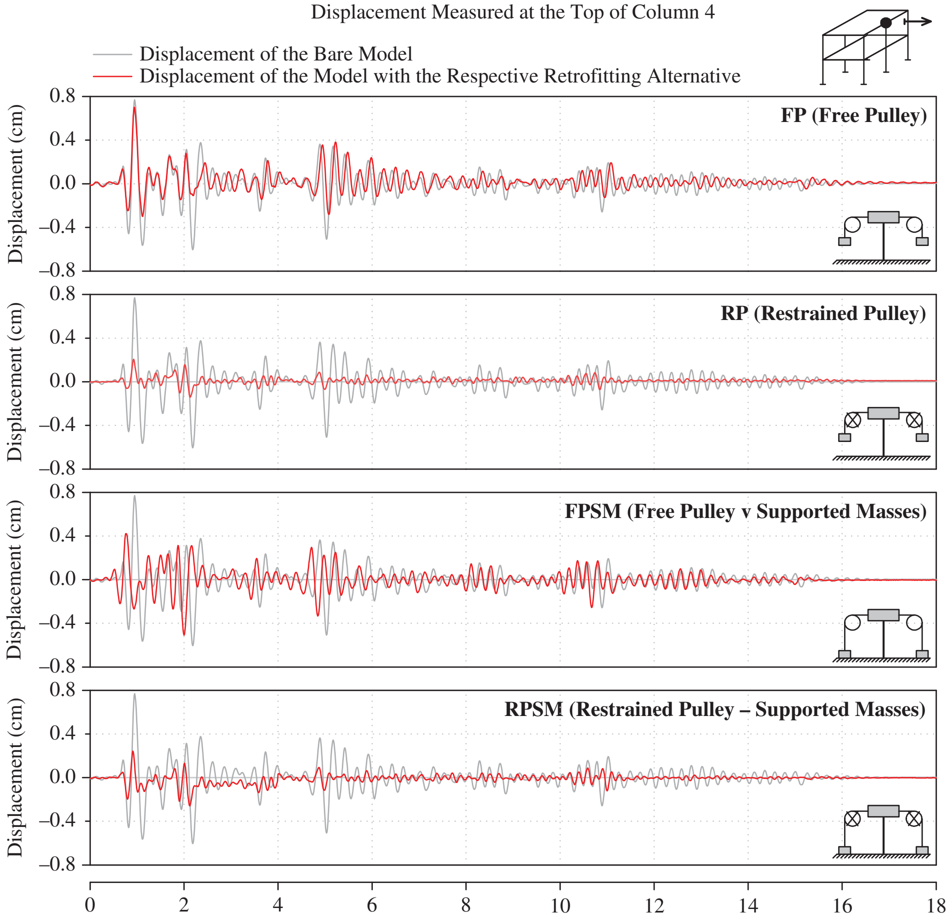

FIGURE 10 Comparison of time displacements during the El Centro tests (color figure available online).

respectively). Similar results were observed for the relative displacements; this is to be expected because the plates supporting the added masses do not provide a rigid diaphragm. However, once the protective systems are installed the situation reverses, i.e., the lateral joints have now higher accelerations. To verify this behavior we created a model of the 3-D frame in the commercial computer program SAP2000. The model was calibrated so that the first and second modes have the same value than those obtained experimentally (see Fig. 7). To simplify the modeling of the friction between the cables and the pulleys, viscous dampers were connected to the central nodes of the second floor. The results obtained from SAP2000 show that the central nodes have indeed higher acceleration than the lateral nodes when the dampers are absent, but as the coefficients of the dampers are increased, the pattern reverses. Moreover, for some of the protective schemes (FP, RSPM) there is a small increment in the peak acceleration as it was pointed out before. This slight increase in the peak acceleration was also observed in the SAP2000 model for some values of the damper coefficients.

Finally, the results in Table 5 and 6 show some asymmetry effects that were also evident in the modal shapes shown before. This is can be attributed to several reasons, such as the enlargement of the shaking table to accommodate the scale mode chosen, a slight skew in the positioning of the model, etc. It is recalled that the shaking table was constructed

TABLE 7 Peak bending moments during the El Centro test

Earthquake	Scheme	Moment in col. 2 (kN.m)	Moment in col. 4 (kN.m)
EL Centro	BM	0.35	0.60
	FP	0.31	0.47
	RP	0.24	0.23
	FPSM	0.23	0.39
	RPSM	0.27	0.27

"in-house" with a limited budget, i.e., it is not a commercial top-of-the-line table. In principle, if one wants to verify a numerical model of a structure or to foretell the actual response of a full-scale existing structure, these asymmetry effects should be avoided or depurated. However, the goal of the research was to establish whether the proposed protective systems were capable of reducing the seismic response, which was indeed the case: obtaining accurate values of the response of the retrofitted structure was not the main objective.

Table 7 presents the peak values of the bending moments at the bottom of column 2 (in the side frame 1 in Fig. 4) and in column 4 (in the central frame 2 in Fig. 4) during the El Centro tests. The table includes the bending moment measured in the original (not retrofitted) structure. Note that all the proposed protective devices were able to reduce the bending moments in the columns. On average, the best reduction in the bending moments was achieved with the RP scheme: 30.8% for column 2 and 61.4% for column 4 measured using the four proposed systems. Figure 11 shows the time variation of the bending moment at the bottom of column 4 and Fig. 12 shows the force vs. displacement curve measured at the cable with the load cell 3 (see Fig. 9) vs. the displacement at the top of the central column measured with the LVDT2 (see Fig. 4). The column of the central frame was the most loaded element in all the tests, and therefore, its bending moment was regarded as the most significant force response quantity to evaluate the effectiveness of the retrofitting alternatives.

Table 8 presents a comparison of the peak accelerations, displacements, and bending moments obtained when the scale model fitted with the RP (fixed pulley) system was subjected to the El Centro ground motion. Two sets of results are presented: one using secondary masses equal to 10% and other considering 5% of the total model mass. It can be noticed that even though the secondary masses were reduced by half, similar reductions in the peak response values were obtained, indicating that this is not a critical factor affecting the performance of the protective system.

Table 9 displays the values of the peak acceleration, displacement, and bending moment at the central column of the scale model (column 4 in Fig. 4) obtained using as base input the scaled accelerograms of the El Centro, Taft, Northridge, and El Salvador earthquakes. The highest reductions in the four response quantities presented are displayed in bold. By examining these values, one can conclude that the best results were again obtained with the RP alternative.

It can be observed that the scale model was able to sustain earthquakes of medium intensity without yielding. The reason for this behavior is that the model was designed taking special precautions so that it behaves within the elastic range. This was done to protect the model and avoid any damage so that it can be used with the different proposed schemes and the five earthquakes ground motions. In any event, the objective of the study was to verify whether the protective systems were able to reduce the response: to preserve the bare and retrofitted model for the different tests we made sure that they had an elastic response.

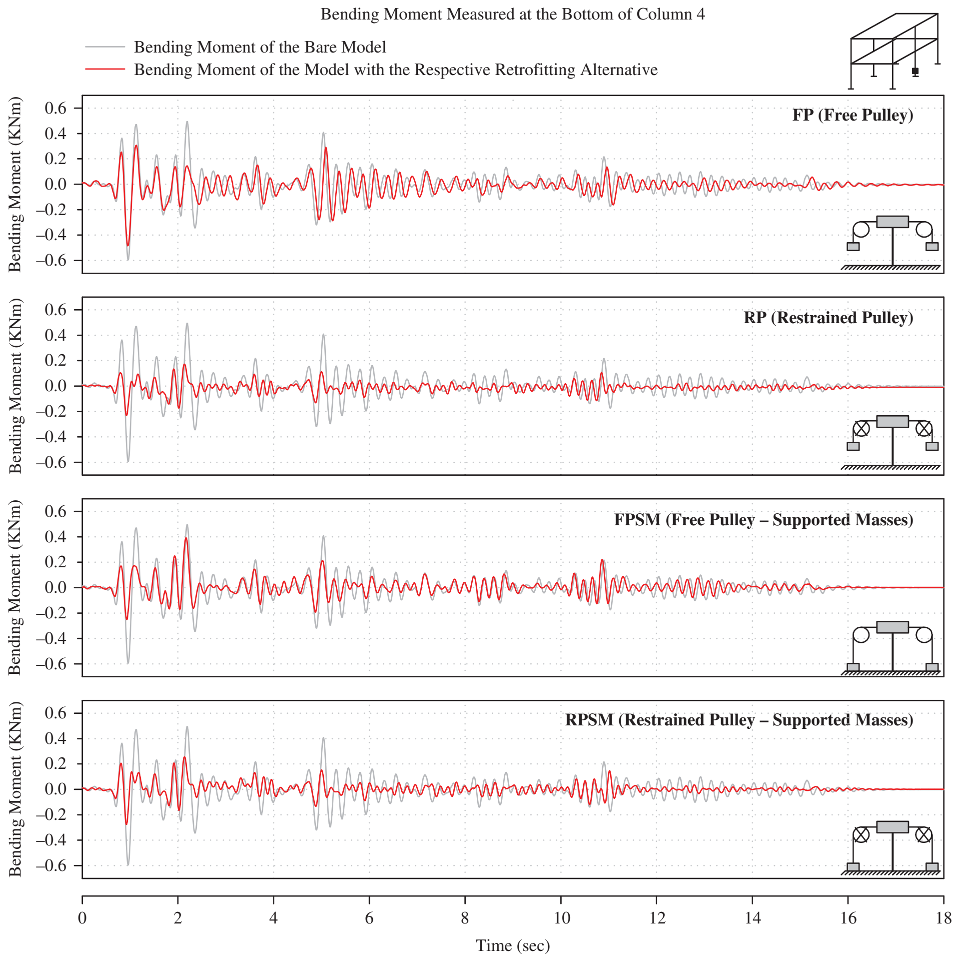

FIGURE 11 Comparison of the bending moments during the El Centro tests (color figure available online).

Figures 13 and 14 show the amplitude of the Frequency Response Function (or transfer function) for the absolute acceleration at the sensor locations A21 and A22 (at the central column of the first and second floor, respectively). The input was the El Centro accelerogram described before. Figure 13 corresponds to the bare model and Fig. 13 is the FRF for the structure fitted with the RP (restrained pulley) scheme. From Fig. 14, one can identify the fundamental natural frequency of the model with the RP protective system. This natural frequency is 6.13 Hz, which is moderately higher than the value of the original structure (4.47 Hz). This higher value was verified with an approximate model created in the program SAP2000. The equivalent damping ratio for the first vibration mode of the retrofitted system is 0.11 whereas for the bare structure the value is 0.01. These are approximate values obtained with the half-power method assuming that the contributions of the higher modes are negligible.

6.3. Effect of the Flexibility of the Beam-Column Connections

As mentioned in a previous section, to consider a structure with deteriorated joints, the beam-column joints of the scale model were designed and constructed as simple (flexible)

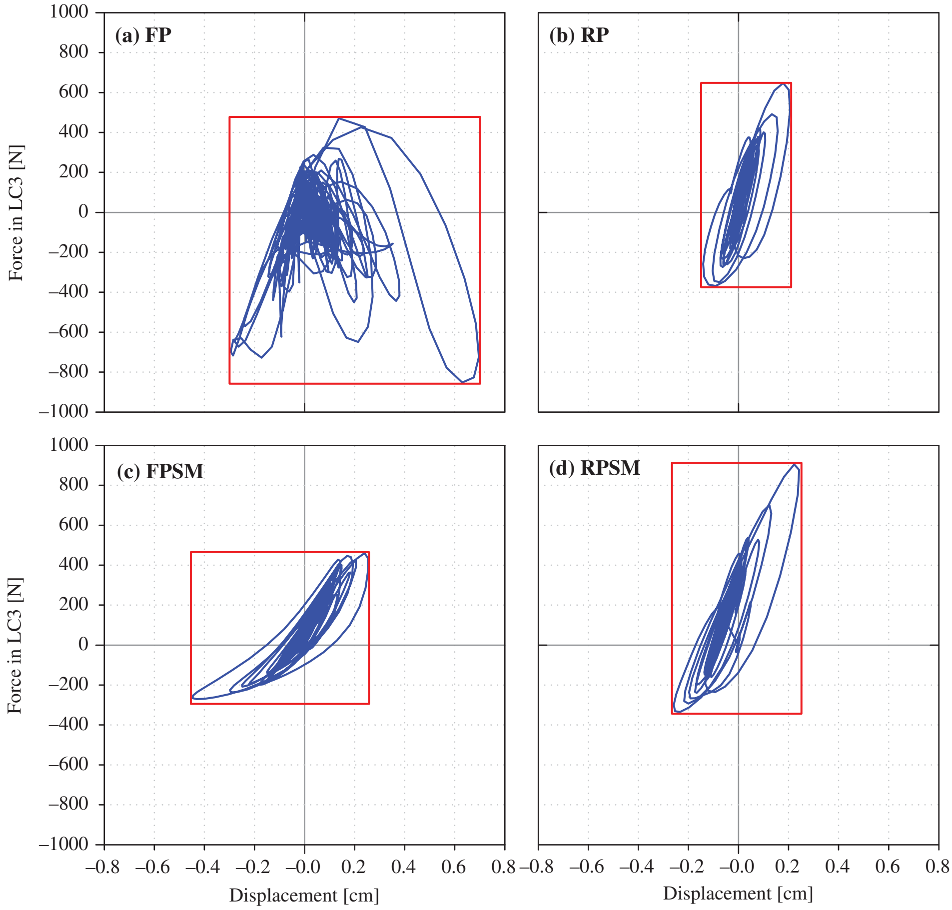

FIGURE 12 Force at load cell 3 vs. displacement at LVDT2 during El Centro Tests (color figure available online).

TABLE 8 Comparison of peak values using RP system with secondary masses of 5% and 10%

Earthquake	Secondary mass (m)	Peak values: Acceleration (A_{22}, %g)	Peak values: Displacement (LVDT2, cm)	Peak values: B. moment (col. 4, KNm)
EL Centro	10%	0.25	0.20	0.23
	5%	0.24	0.28	0.27

connections which are assumed to be free to rotate. However, it is interesting to assess the performance of the proposed protective systems if the connections were stiffer (i.e., partially or fully restrained connections). This was done by means of numerical simulations using the structural analysis program SAP2000 Version 14.1. A model of the main and secondary structures tested in the lab was created in SAP2000 and is shown in Fig. 15. The first model created in SAP2000 was the same as the model tested, i.e., with pinned connections. Although initially the same geometry, cross sections of beams and columns, added

TABLE 9 Peak acceleration, displacement, and bending moment at column 4 (in the central frame) obtained with the four earthquake motions

Earthquake	Scheme	Acceleration at level 1 A_{21} (%g)	Acceleration at level 2 A_{22} (%g)	Displacement at level 2 Displ. (cm)	Moment at bottom of column 4 M (KNm)
EL Centro	BM	0.18	0.47	0.76	0.60
	FP	0.15	0.34	0.71	0.47
	RP	0.19	0.25	0.20	0.23
	FPSM	0.15	0.28	0.46	0.39
	RPSM	0.23	0.34	0.25	0.27
Taft	BM	0.16	0.37	0.64	0.52
	FP	0.16	0.35	0.64	0.47
	RP	0.15	0.23	0.18	0.22
	FPSM	0.15	0.32	0.30	0.24
	RPSM	0.17	0.25	0.18	0.22
Northridge	BM	0.16	0.34	0.56	0.42
	FP	0.13	0.30	0.43	0.33
	RP	0.15	0.20	0.13	0.18
	FPSM	0.16	0.31	0.28	0.27
	RPSM	0.17	0.25	0.18	0.20
San Salvador	BM	0.16	0.46	0.81	0.60
	FP	0.14	0.44	0.61	0.47
	RP	0.19	0.28	0.28	0.27
	FPSM	0.18	0.38	0.58	0.46
	RPSM	0.22	0.33	0.30	0.31

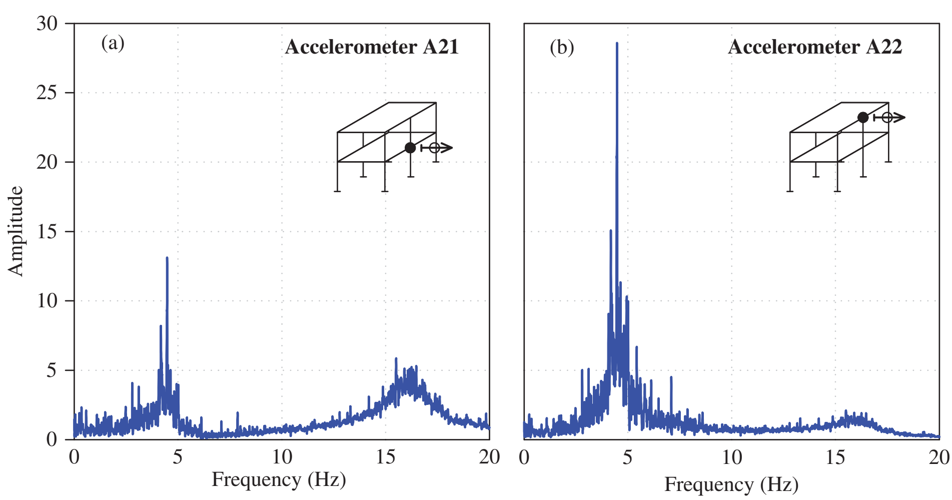

FIGURE 13 Frequency Response Function for the acceleration of the central column of the bare model: (a) at the first floor; and (b) at the second floor (color figure available online).

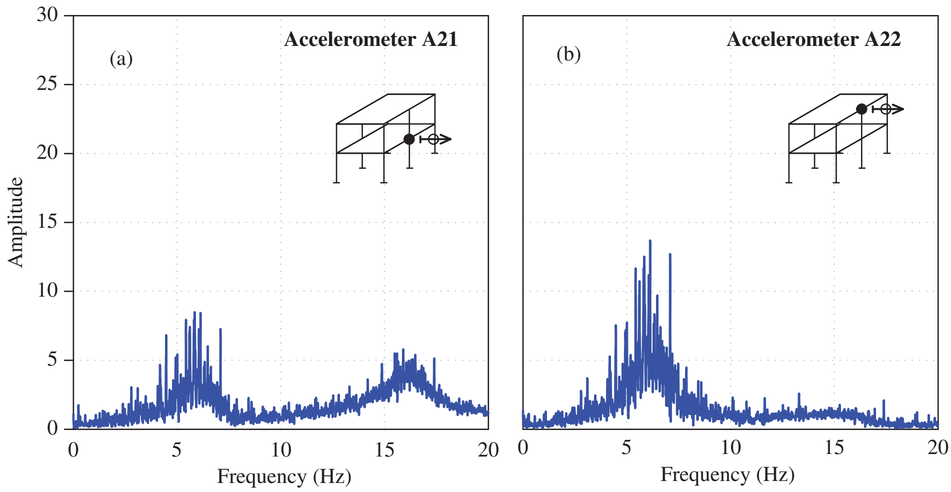

FIGURE 14 Frequency Response Function for the acceleration of the central column of the model with the RP system: (a) at the first floor; and (b) at the second floor (color figure available online).

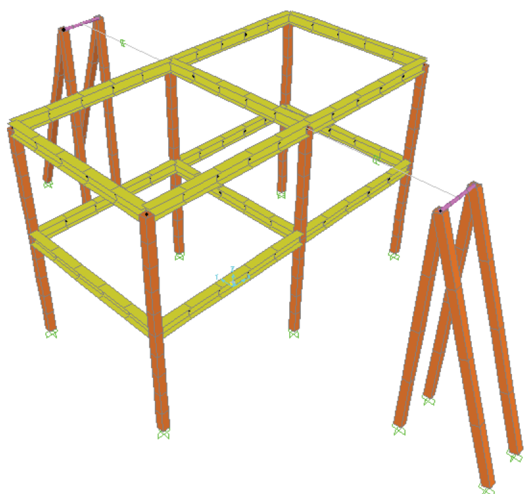

FIGURE 15 Numerical model of the main and supporting structures in SAP2000 (color figure available online).

masses, cable diameters, etc., of the scale model were used to define the SAP2000 model, some minor changes were subsequently introduce so that both have the same lower natural frequencies. The damping was also updated so that the two models had analogous acceleration time histories when subjected to the scaled El Centro record. Next, the numerical model was modified to include rigid beam-column connections.

The SAP2000 models were subjected to the El Centro acceleration record. The top graphs in Fig. 16 show the time variation of the accelerations at the top of the building for the original model (i.e., without the protective system) and for the structure fitted with the Restrained Pulley system. The lower graphs display similar responses but now for the bare and retrofitted model with rigid connections. It can be seen that the level of response

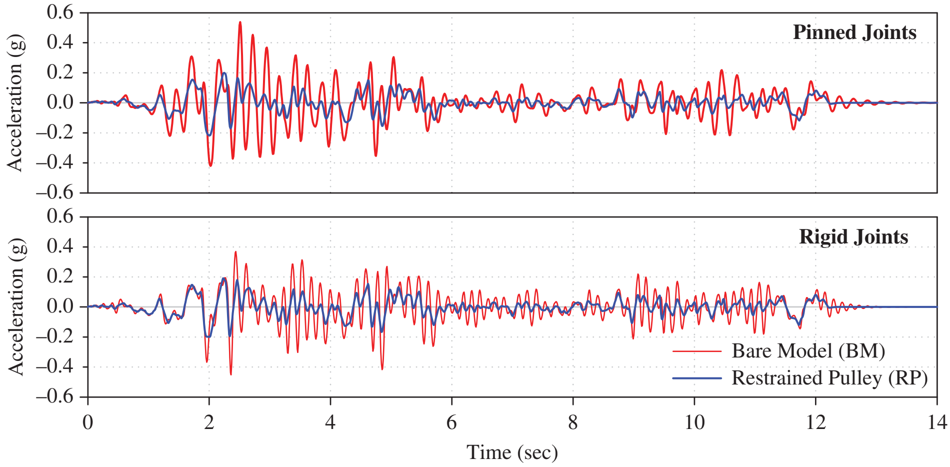

FIGURE 16 Variation of floor accelerations from the numerical model with pinned (top) and rigid connections (bottom) (color figure available online).

reduction (at least in the acceleration) is comparable. For the simple connections case the peak acceleration was reduced by 58.5%, whereas for the moment connections case the corresponding response reduction is 55%.

7. Summary of Results

To summarize the most important findings of the experimental program undertaken to assess the performance of the four protective devices and to help to establish conclusions, a graphical synopsis is presented in Fig. 17. The figure shows the reduction in the peak acceleration and displacement at the top of the central column and the bending moment at its bottom as a percentage of the response of the original structure (indicated as the Bare Model). The four earthquake ground motions with a 0.3 g PGA are considered. The following observations can be made by inspecting the results presented in Fig. 17.

1. All the protective systems were able to reduce the measured response quantities reported in Fig. 15a due to the four earthquakes, except for the top displacement of the structure equipped with the FP device under the Taft ground motion.
2. The best results in terms of response reduction were achieved using those passive systems in which friction between the cable and the pulleys developed.
3. The best reduction in the acceleration measured by the accelerometer A22 located at the top of the central column was obtained with the RP system, as shown in Fig. 16a. The measured acceleration peaks were between 53% and 62% of the values recorded in the bare model. However, in some cases a minor increase in the peak acceleration was measured at other nodes (see Table 5).
4. As it can be seen in Fig. 16b, the largest reductions in the maximum relative displacements were obtained with the RP scheme: they were between 23% and 34% of the respective values for the bare model. The next most efficient system for displacement abatement was the RPSM, which reduced the displacements between 28% and 38%. Although not shown in Fig. 16, the tests demonstrated that the displacements at other locations were also reduced by the protective systems.
5. The best reductions in the bending moment at the base of column 4 were achieved by the RP and RPSM schemes, as shown in Fig. 16c. The maximum moments measured in the model with the RP system have values between 39% and 45%

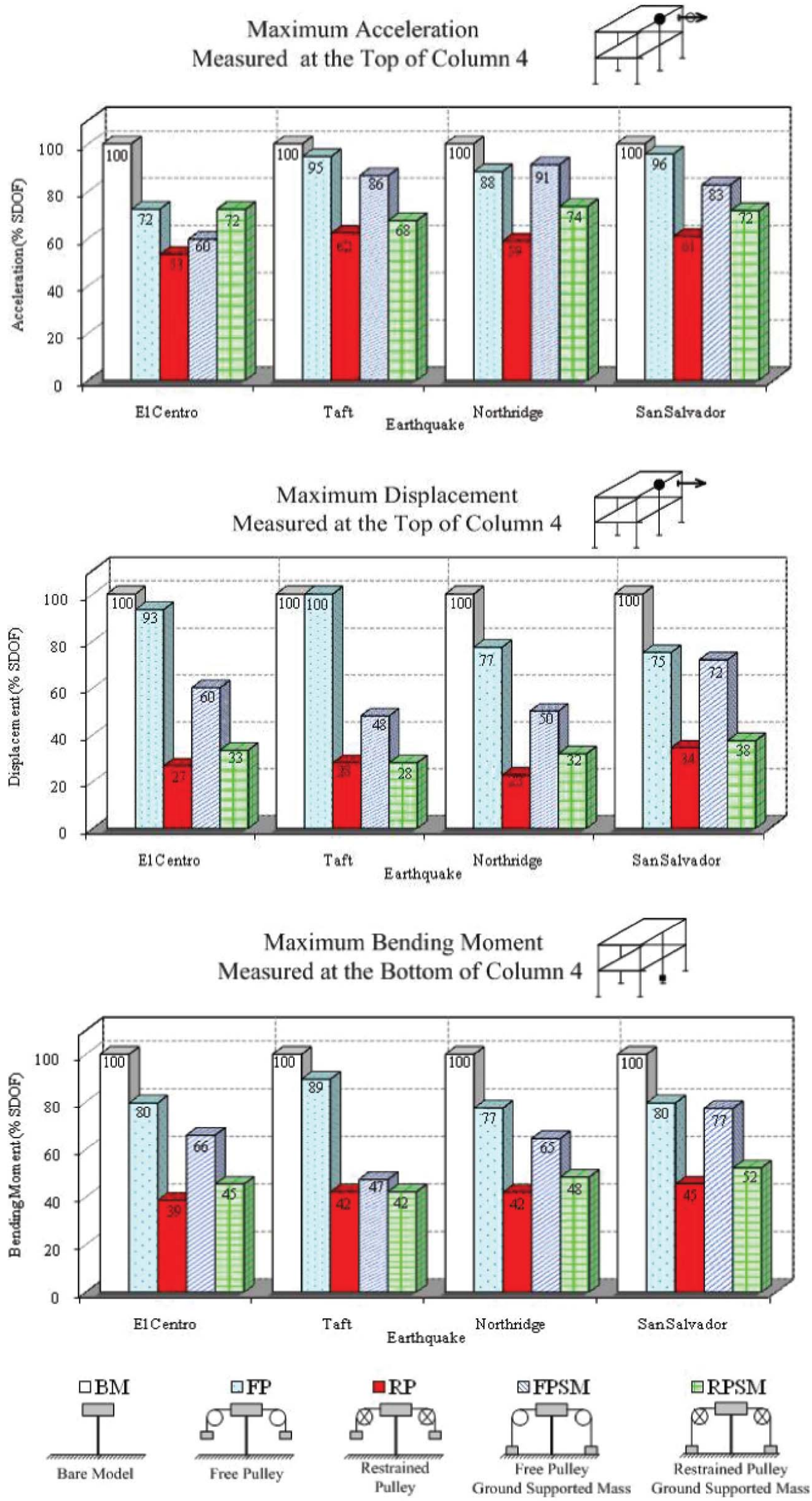

FIGURE 17 Results from simulated earthquake tests as a percentage of bare model response (color figure available online).

lower than those in the original structure. For the RPSM system, the second best alternative, the reductions achieved ranged from 42–52%.

6. The experimental results obtained by retrofitting the scale model with the RP system showed that there is no significant difference in the response reduction when the total secondary masses were reduced from 10% to 5% of the total mass.

8. Practical Considerations

The architectural impact of the proposed devices was not addressed in this article. The research project conducted and presented in the article was conceived as a proof-of-concept. Therefore, the arrangement used in the project consisting of a secondary structure beside the main structure was devised to facilitate the construction and testing of the different schemes. In practice, the scheme could be implemented by using an internal or external core, or it can be erected into an inner court, if available. For example, the proposed arrangements can be incorporated into an internal core not attached to the building, as shown in Fig. 18. Otherwise, the building can be designed with reentrances in which the frame and the devices can be accommodated (see Fig. 19a). If the building is already constructed, the proposed system can be accommodated into salients as shown in Fig. 19b. These entrances and salients can be covered with architectural features for aesthetic purposes. In addition,

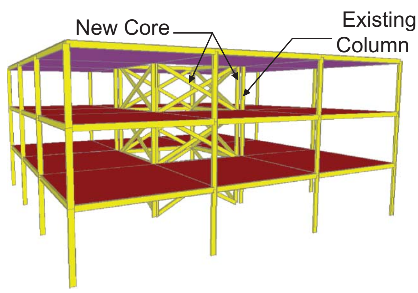

FIGURE 18 Protective system set up in an internal core (color figure available online).

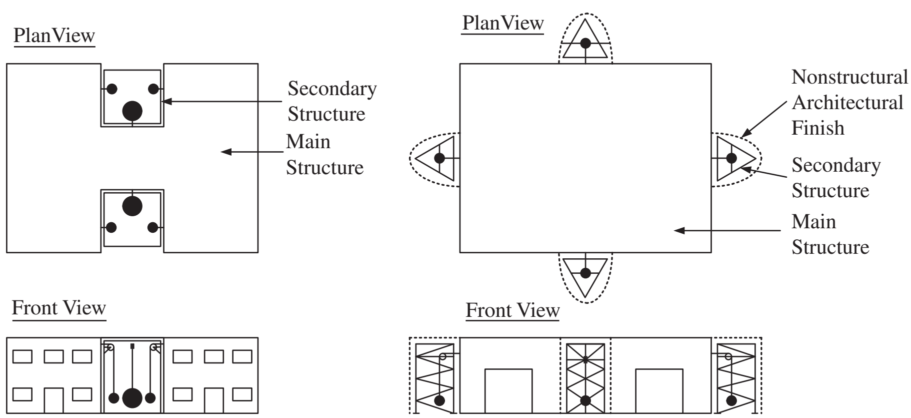

FIGURE 19 Protective system installed in: (a) reentries of the structure; (b) outside the building plant.

it may not be necessary to apply the protective system in the two orthogonal directions (as shown in the figures), but rather in the direction which needs retrofitting. These are just preliminary propositions that in practice should be given proper and more careful considerations including costs, architectural feasibility, etc.; however, these topics are beyond the scope of this article.

It is acknowledged that the proposed protective system is not intended for every possible application because of the (external or internal) space requirements. It can, however, be particularly useful when the retrofitting scheme cannot interfere with the internal circulation. Moreover, the system can also suitable for buildings where the retrofitting work cannot disrupt the normal operations due to the very high cost associated with idle times (this is the case, for example, of the manufacturing plants for the pharmaceutical industry).

There are also a number of potential implementation issues dealing with the FPSM and RPSM schemes (the alternative with the impacting masses) that were pointed out by the reviewers of the article. One of them is the noise caused by the mass impacting the ground. Although in principle this could be a nuisance, it is not expected to be a concern compared to the commotion caused by a strong earthquake. Another potential matter of consideration is that the impact of the masses may affect the foundation. However, the impact will take place outside the building and will not hit directly above the foundation. In any case, the effect of the impact can be diminished by embedding the masses in a tube with a highly viscous liquid. Nevertheless, in its current form the FPSM and RPSM schemes gave results which were inferior to those obtained with the other alternatives studied and thus it was not deemed pointful to carry out further studies of these issues.

9. Conclusions

The results presented in this article are a first attempt to assess the effectiveness of the four proposed passive protective system as means to reduce the seismic response of steel buildings. Two of the systems showed promising capabilities in this regard: the RP (Restrained Pulley) and the RPSM (Restrained Pulley with Ground Supported Mass) systems. These two protective systems should be further studied to confirm its effectiveness, in particular the RP scheme which does not have the potential drawback of a mass hitting the ground. In this regard, the experimental study carried out and described in this article should be considered as a proof-of-concept.

The tests performed had some limitations due to restrictions imposed by the size and other capabilities of the shaking table. More comprehensive tests using larger models should be performed. In addition, numerical models that simulate the behavior of the most promising protective schemes should be developed. Finally, a cost analysis should be undertaken to compare the cost associated with these retrofitting alternatives compared to others methodologies, such as friction and viscous dampers.

Finally, before the recommended protective systems can be implemented in real structures, some design guidelines are necessary. For instance, it is necessary to select the size of the pulleys and the cross-section of the cables to achieve a certain response reduction (so far, only the mass of the device was established). This requires having a numerical model of the protective system to examine the effect of these parameters on the response reduction achieved. The work described in this article had the goal of assessing the performance of the protective devices, i.e., it was a proof-of-concept project as mentioned before. We are currently working on simple analytical/numerical model that will shed light on the engineering of the device; the results will be presented in a future publication.

References

Aiken, I. D., Nims, D. K., Whittaker, A. S., and Kelly, J. M. [1993] "Testing of passive energy dissipation systems," *Earthquake Spectra* **9**(3), 335–370.

Bracci, J. M., Reinhorn, A. M., and Mander, J. B. [1992] "Seismic resistance of reinforced concrete frame structures designed only for gravity loads. Part I: design and properties of a one-third scale model structure," *Technical Report NCEER-92-0027*, National Center for Earthquake Engineering Research, Buffalo, New York.

Cheng, F. Y., Jiang, J., and Lou, K. [2008] *Smart Structures: Innovative Systems for Seismic Response Control*, CRC Press, Boca Raton, Florida.

Christopoulos, C. and Filiatrault, A. [2006] *Principles of Passive Supplemental Damping and Seismic Isolation*, IUSS Press, Pavia, Italy.

Cortés-Delgado, M. D. [2005] "Development of the UPRM earthquake simulator facility for dynamic model analysis," Masters of Science Thesis, Civil Engineering Department, University of Puerto Rico at Mayagüez, Puerto Rico.

Hanson, R. D. and Soong, T. T. [2001] *Seismic Design with Supplemental Energy Dissipation Devices*, EERI Monograph No. 8, Earthquake Engineering Research Institute, Oakland, California.

Kohan, P. H. [2007] "Study of the seismic behavior of steel buildings with a 1/6 scale model and shaking table tests," Masters of Science Thesis, Civil Engineering Department, University of Puerto Rico at Mayagüez, Puerto Rico.

Martínez-Cruzado, J. A., Irizarry-Padilla, J., and Portela-Gautier, G. [2001] "Espectros de diseño para las ciudades principales de Puerto Rico basado en registros de aceleraciones Mundiales," *Revista Internacional de Desastres Naturales, Accidentes e Infraestructura Civil* **1**(1), 21–31.

Mills, R. S., Krawinkler, H., and Gere, J. M. [1979] "Model tests on earthquake simulators; development and implementation of experimental procedures," *Report N° 39*, The John A. Blume Earthquake Engineering Center, Dept. of Civil Engineering, Stanford University, Stanford, California.

Moncarz, P. D. and Krawinkler, H. [1981] "Theory and application of experimental model analysis in earthquake engineering," *Report N° 50*, The John A. Blume Earthquake Engineering Center, Department of Civil Engineering, Stanford University, Stanford, California.

Soong, T. T. [1990] *Active Structural Control: Theory and Practice*, Longman/Wiley, London/New York.

Soong, T. T. and Dargush, G. F. [1997] *Passive Energy Dissipation Systems in Structural Engineering*, John Wiley, London.

Soong, T. T. and Spencer Jr., B. F. [2002] "Supplemental energy dissipation: state-of-the-art and state-of-the-practice," *Engineering Structures* **24**(3), 243–259.

Spencer Jr., B. F. and Nagarajaiah, S. [2003] "State of the art of structural control," *Journal of Structural Engineering* **129**(7), 845–856.